Iterative Decoding of Convolutionally Encoded Signals Over Multipath Rayleigh Fading Channels

Antoine O. Berthet, *Member, IEEE*, Berna Sayrac Ünal, *Member, IEEE*, and Raphaël Visoz

***Abstract*—In this paper, we analyze and compare several strategies for iteratively decoding trellis-encoded signals over channels with memory. Soft-in/soft-out extensions of reduced-complexity trellis search algorithms such as delayed decision-feedback sequence estimating (DDFSE) or parallel decision-feedback decoding (PDFD) algorithms are used instead of conventional BCJR and min-log-BCJR algorithms. It has been shown that for long channel impulse responses and/or high modulation orders where the BCJR algorithm becomes prohibitively complex, the proposed algorithms offer very good performance with low complexity. The problem of channel estimation in practical implementation of turbo detection schemes is studied in the second part. Two methods of channel reestimation are proposed: one based on the expectation-maximization (EM) algorithm and the second on a simple Bootstrap technique. Both algorithms are shown to dramatically improve the performance of the classical pseudo-inverse channel estimation performed initially on a training sequence.**

***Index Terms*—Bootstrap algorithm, delayed decision-feedback estimation (DDFSE), expectation-maximization (EM) algorithm, iterative decoding, parallel decision-feedback decoding (PDFD), turbo detection, turbo reestimation.**

I. Introduction

SINCE their first presentation in 1993 [1], a considerable amount of work has been done on turbo codes, both for improving the original scheme and for better understanding the reasons for their astonishing performances. Moreover, the "turbo principle" has been extended to many fields other than channel coding theory and should now be regarded as a general approach for combining and serially performing in an iterative fashion two or more tasks in the receiver digital communication chain. In the past few years, a new concept, called "turbo equalization," has emerged as a way of efficiently fighting against strong channel InterSymbol Interference (ISI) caused by limited bandwidth, multipath propagation, and motion [2]. Such a concept is potentially very attractive for time division multiple access (TDMA) schemes with enhanced data rates such as enhanced data rates for global systems for mobile communications [3] (GSM) and Evolution (EDGE) [4], [5]. The basic idea consists of considering the channel as a time-varying nonrecursive nonsystematic convolutional code. Assuming an outer convolutional channel encoder and a channel interleaver, the reference turbo detection scheme (scheme 1) is then formally analogous to a serial concatenation of convolutional codes and the same iterative techniques can be applied to realize joint detection and decoding [13]. Performing iterations like in turbo decoding can improve the bit error rate (BER) and the frame error rate (FER) dramatically. In fact, simulations show that all the ISI can be eliminated by such a process and the performance of coded signals over the Gaussian channel can be reached assuming perfect channel estimation and sufficient interleaver depth.

From the analysis of studies about turbo detection concept, three major issues can be identified. This paper aims at bringing sketches of solutions to each of them.

In the original paper describing the turbo detector [2], a min-log-BCJR algorithm was used for symbol detection and a low-complexity SOVA for channel decoding [6]. More recently, in [8], optimal symbol-by-symbol BCJR detectors and decoders have been introduced to improve the scheme [10]. Unfortunately, the complexity of all those MAP or sub-MAP devices might become quickly prohibitive when higher level modulations rather than simple BPSK (or GMSK) and 6-tap (or more) channel impulse responses are considered. Moreover, symbol detection task is repeated several times during the iterative process. Consequently, the first challenge is the reduction of the overall computational complexity of the turbo detector. Since this complexity will be dominated by the ISI decoder, we focus on the design of a low-complexity turbo detector based on a suboptimal soft-input/soft-output delayed decision-feedback sequence estimator (SISO-DDFSE), coupled with a minimum-phase prefiltering. We show that its performance remains close to optimal for the TU3 channel profile [17], [18].

The second attractive problem studied here deals with an improvement of the previous reference scheme, by combining detection and powerful iteratively decodable codes, as first suggested in [11], keeping in mind the intuitive idea that the better the channel encoder is, the better the overall turbo detector performance will be. It has been shown in [13] that serially concatenated codes (SCCC) could be more efficient than parallel concatenated ones (PCCC). In particular, SCCC do not suffer from error floor phenomenon and consequently appear as the most suitable candidates for low BER data applications. This is essentially the reason why we focus on SCCCs in this paper, even though other powerful code combinations can also be investigated (see for example [12]). The main part of the article is devoted to the design of two different schemes involving the SCCC and to the analysis of their iterative decoding. The first scheme (scheme 2) is made of an SCCC, concatenated with the

Manuscript received April 20, 2000. This paper was presented in part at Globecom2000, San Francisco, CA. This work was done at France Telecom Research and Development, 92794 Issy Les Moulineaux, France.

A. O. Berthet is with Alcatel Space Industries, 92000 Nanterre, France.

B. S. Ünal is with Middle East Technical University, 06531 Inonu Bulvari, Ankara, Turkey.

R. Visoz is with France Telecom R&D, 92794 Issy Les Moulineaux, France.

Publisher Item Identifier S 0733-8716(01)03911-7.

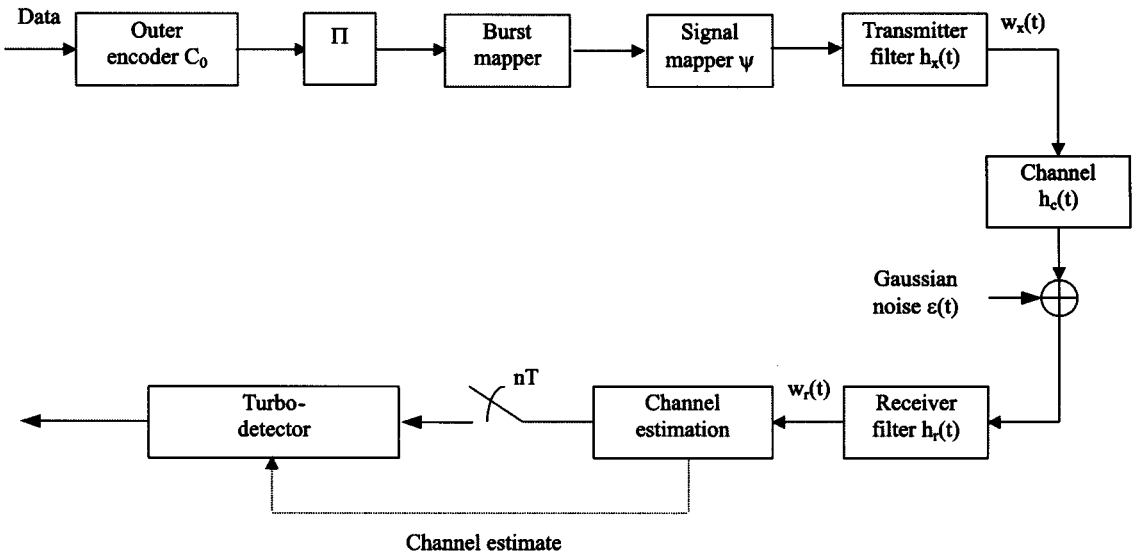

Fig. 1. Transmission reference scheme.

ISI channel code. In this approach, all codes are separated by pseudo-random interleavers. Assuming a constant spectral efficiency, the modulation order must be increased to counterbalance the inner code rate. Scheme 2 is, in fact, formally equivalent to a doubly serially concatenation of convolutional codes [16] and can be decoded in the same way. Due to modulation order increase, however, detection task will be computationally cumbersome, even with the suboptimal DDFSE algorithm.

To overcome this problem, a last scheme (scheme 3) will be finally presented, as a more interesting low-complexity fashion to introduce additional coding gain. It will involve an outer convolutional code concatenated with a trellis coded modulation (TCM). A SISO parallel decision-feedback decoder (SISO-PDFD) [22], [23] will be used to perform joint detection and decoding on the TCM trellis only. It will be shown that such a suboptimal approach gives similar and sometimes better results than previous ones with a far smaller complexity.

To conclude with the turbo detection analysis, the problem of channel knowledge also has to be raised and carefully investigated. In [9] indeed, it is shown by simulations that MAP and sub-MAP devices are very sensitive to channel estimation. A degradation of 2.9 dB occurs when assuming mismatched channel estimation by classical technique (i.e., pseudo-inverse method on constant amplitude zero autocorrelation training sequence). We propose here at least two methods for reestimating the channel coefficients. The first method exploits the EM algorithm. Tne EM iteration is done after each turbo detector iteration. The second method is even more simple and basically consists of a simple bootstrap process using linear pseudo-inverse. A significant part of the degradation introduced by mismatched channel estimation can be recovered by such reestimation methods, without substantial complexity increase. It must be emphasized that the turbo detection coupled with a channel reestimation can be fairly compared with the ISI cancellation based turbo equalization proposed by [7] where mismatched channel estimation is assumed. Simulations prove that the former achieve far better results than the latter for a wide range of tested schemes.

The paper is organized as follows: Section II is devoted to scheme 1 where the transmission reference model is described, the turbo detection principle is reviewed, and the SISO-DDFSE is derived. In Section III, scheme 2 is considered where iterative detection and SCCC decoding is described. Section IV covers scheme 3 which performs iterative detection and decoding of an outer code concatenated with TCM by using the SISO-PDFD algorithm. In Section V, the performances of the proposed schemes are given through computer simulations. Section VI is devoted to the problem of channel reestimation where the EM and the Bootstrap algorithms are derived, and the performances of these proposed algorithms are given. Finally, in Section VII concluding remarks and future research topics are presented, and the Appendix outlines the derivation of the EM channel reestimation algorithm.

II. Low Complexity Turbo Detection

A. Transmission Reference Model

Let us consider the digital communication transmission chain depicted on Fig. 1. A data sequence $\underline{d}_1^{\tau_o} = \{\underline{d}_1, \ldots, \underline{d}_{\tau_o}\}$ of τ_o symbols enters an outer channel encoder C_o, which produces a coded sequence $\underline{c}_1^{\tau_o} = \{\underline{c}_1, \ldots, \underline{c}_{\tau_o}\}$. Each data symbol $\underline{d}_n = [d_{n,1}, \ldots, d_{n,k_o}]$ contains k_o bits, whereas each coded symbol $\underline{c}_n = [c_{n,1}, \ldots, c_{n,n_o}]$ contains n_o bits.

Coded bits are interleaved by a pseudo-random interleaver Π and divided into N bursts $\underline{a}_1^{\tau} = \{\underline{a}_1, \ldots, \underline{a}_{\tau}\}$ of τ bit-labeled symbols, including known symbols for channel estimation and synchronization purposes together with tail and guard symbols. To each symbol $\underline{a}_n = [a_{n,1}, \ldots, a_{n,q}]$, a $Q = 2^q$-ary signal mapper Ψ associates a complex-valued symbol z_n. The transmitter produces the complex base-band waveform

$$w_x(t) = \Re e\left\{\sum_n z_n h_x(t - nT)\right\} \tag{1}$$

where $h_x(t)$ denotes the base-band complex impulse response of the lowpass equivalent transmitter filter and $1/T$ is the

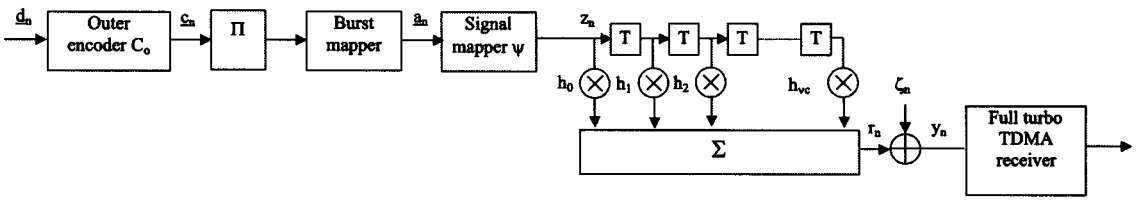

Fig. 2. Equivalent discrete-time model of the reference scheme.

symbol rate. At reception, the received base-band signal is given by

$$w_r(t) = \sum_n z_n g(t - nT) + \epsilon'(t) \tag{2}$$

where the complex impulse response $g(t)$ takes into account the transmitter and receiver filters, together with the dispersive channel. $\epsilon'(t)$ denotes the convolution of the complex zero-mean Gaussian noise $\epsilon(t)$ (of single-sided power spectral density N_0) with the receiver filter $h_r(t)$. The signal is then sampled at rate $1/T$ in conjunction with channel estimation (thanks to the training sequence) to yield N infinite quantized received bursts $y_1^\tau = \{y_1, \ldots, y_\tau\}$ and the channel estimate, which feed the turbo detector.

B. Equivalent Discrete-Time Model and Associated Trellis

We represent in Fig. 2 the equivalent discrete-time model (scheme 1) made of an encoder C_o, an interleaver Π, a signal mapper Ψ, and a transversal filter $\mathfrak{H}(z)$ with $(\nu_c + 1)$ dimensionnal complex vector $\underline{h} = [h_0, h_1, \ldots, h_{\nu_c}]$. At the output of the equivalent discrete-time channel (including transmit and receive filters), received samples are given by

$$y_n = h_0 z_n + \sum_{k=1}^{\nu_c} h_k z_{n-k} + \zeta_n \tag{3}$$

where $\sum_{k=1}^{\nu_c} h_k z_{n-k}$ represents the ISI introduced by the channel and ζ_n the (considered uncorrelated) complex Gaussian noise samples of variance $2\sigma^2$. ζ_n is a circularly symmetric complex Gaussian variable (i.e., its real and imaginary parts are uncorrelated and of same power σ^2).

As is well known, the equivalent discrete-time ISI channel can be regarded as a nonrecursive nonsystematic convolutional code with memory ν_c and rate-1, whose single complex-valued generator polynome may vary in time. The time progression of the states, as well as the possible transitions, can be visualized by a regular trellis diagram $T(S, B)$. Note that, in the following, the channel estimation is considered valid for the whole burst duration (i.e., the channel is assumed (quasi)-stationary for a burst duration). We denote by S_n and B_n state and branch spaces at depth and section n, respectively. Due to time-invariant property, state and branch space complexities satisfy

$$|S_n| = Q^{\nu_c}, \qquad \forall n \in [0, \tau]$$

and

$$|B_n| = Q^{\nu_c + 1}, \qquad \forall n \in [1, \tau]. \tag{4}$$

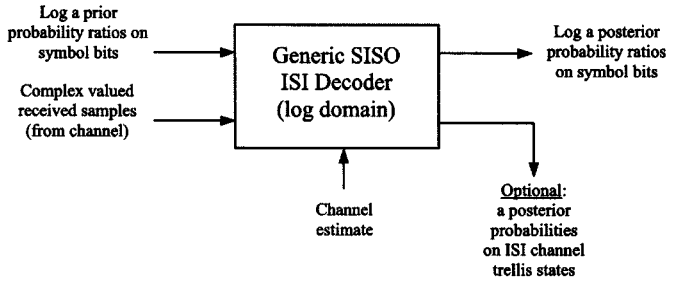

Fig. 3. A generic log-BCJR equalizer.

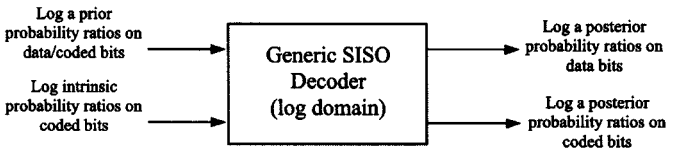

Fig. 4. A generic log-BCJR decoder.

Optimally, the detection must be performed using the optimal symbol-by-symbol BCJR algorithm [10], [8], which operates on the full ISI channel trellis and whose complexity is roughly in $O(|B|)$. A generic ISI decoder module is shown in Fig. 3.

C. Turbo Detection Principle

Similarly, the channel code can be optimally decoded using the BCJR algorithm. A generic log-BCJR decoder module is depicted in Fig. 4. Inputs and outputs are supposed *a posteriori* probability (APP) ratios on bits (converted in the logarithmic domain) conditioned or not by the knowledge of the considered code. From delivered APPs on each bit of a sequence, an extra knowledge, called extrinsic information, is drawn, which basically consists of the incremental information about that particular bit brought by information available from all other bits through the decoding process. The basic SISO module has been extensively described (see [14], [15], and [9]).

We now recall the turbo detection principle (Fig. 5). The SISO ISI decoder delivers log *a posteriori* probability (log-APP) ratios on bits $a_{n,j}$ of symbols $\underline{a}_n$ composing burst $\underline{a}_1^\tau$, aided with log *a priori* probability ratios on them coming from the decoder (null at the beginning) and given the received burst y_1^τ and an estimate (or a reestimate) $\hat{\underline{h}}$ of the channel coefficient vector. As we will show thereafter, those log-APP ratios on bits can be divided in two parts according to the following:

$$\lambda(\mathbf{a}_{n,j}) = \lambda_a(\mathbf{a}_{n,j}) + \lambda_e(\mathbf{a}_{n,j}). \tag{5}$$

After deinterleaving Π^{-1}, the overall sequence of log extrinsic probability ratios becomes a sequence of log *intrinsic* probability ratios on bits of coded symbols for the channel

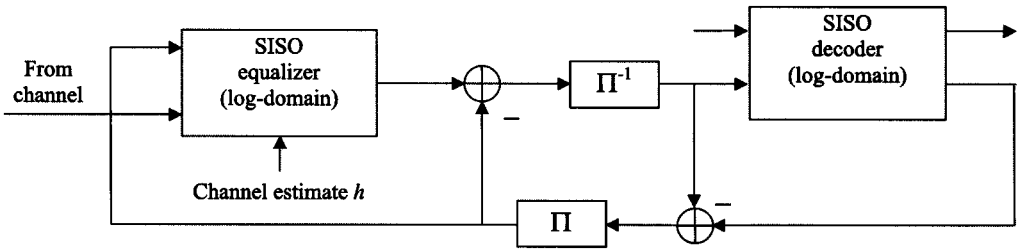

Fig. 5. Turbo detection principle.

decoder. Similarly at the output of the SISO channel decoder, each log-APP ratio on coded bit $\lambda(c_{n,j})$ can be split into an intrinsic part and an extrinsic part. The latter can be computed by subtracting bitwise the log *a priori* ratio $\lambda_a(\mathbf{c}_{n,j})$ at the input of the decoder from the corresponding log-APP ratio $\lambda(\mathbf{c}_{n,j})$ at the output, so that

$$\lambda_e(\mathbf{c}_{n,j}) = \lambda(\mathbf{c}_{n,j}) - \lambda_a(\mathbf{c}_{n,j}). \tag{6}$$

Sequence of log extrinsic probability ratios on coded bits is reinterleaved and passed to the SISO ISI decoder as N new sequences (one per burst) of log *a priori* probability ratios on bits of bit-labeled symbols for a next detection attempt. Iterating the procedure a few times leads to a dramatic improvement of the final BER and FER on data bit sequence.

D. SISO DDFSE Detector

To reduce the overall turbo detection complexity, suboptimal trellis-based detectors must be introduced. Among the set of trellis-based reduced-states sequence estimators [21], the DDFSE appears as the most suitable candidate because of its high regular Viterbi-like structure and the good performance it provides in regard with its moderate complexity [19]. For a positive integer ν_r, we say that a trellis input sequence $\underline{a}_1^n$ ends at substate s if $\underline{a}_1^n$ terminates with the substring $s = \underline{a}_{n-\nu_r+1}^n$. ν_r is called the reduced memory. At any depth n, the substate space S_n coincides with the full BCJR trellis state space S_n if $\nu_r = \nu_c$. In the case where $\nu_r < \nu_c$, S_n is reduced to the subset of S_n made of all possible substates s derived from full states s, so that

$$|S_n| = Q^{\nu_r}, \qquad \forall n \in [0, \tau]$$

and

$$|B_n| = Q^{\nu_r+1}, \qquad \forall n \in [1, \tau]. \tag{7}$$

The above formalism applies for the definition of the subtrellis $T(S, B)$ on which the DDFSE algorithm proceeds. At each section, and for all transitions, the branch metric computation involves a convolution of the channel discrete-time impulse response with a sequence of $\nu_c + 1$ already estimated symbols. Only the first ν_r estimated symbols for that sequence are available on the current studied transition and on the departure subtrellis substate with which it is connected.

In all of the following derivations, bold letters indicate random variables, whereas normal letters indicate possible realizations. At each time index $n \in [1, \tau]$ and for all bit indexes $j \in [1, q]$, the optimal symbol-by-symbol BCJR algorithm would compute the log APP ratio, defined as

$$\lambda(\mathbf{a}_{n,j}) = \ln \frac{\Pr\left(\mathbf{a}_{n,j} = 1 \middle| y_1^\tau, \hat{\underline{h}}\right)}{\Pr\left(\mathbf{a}_{n,j} = 0 \middle| y_1^\tau, \hat{\underline{h}}\right)} \tag{8}$$

where $\hat{\underline{h}}$ is an estimate (or a reestimate) of the transverse channel coefficient vector (possibly turned into minimum phase), and y_1^τ is an observed sequence of length τ. In the following derivation, the conditioning by $\hat{\underline{h}}$ is implicit and omitted for the ease of expressions.

Marginalizing on bit-labeled input symbol sequences (8) can be rewritten as

$$\lambda(\mathbf{a}_{n,j}) = \ln \frac{\sum_{\underline{a}_1^\tau, a_{n,j}=1} p(a_1^\tau, y_1^\tau)}{\sum_{\underline{a}_1^\tau, a_{n,j}=0} p(a_1^\tau, y_1^\tau)} \tag{9}$$

where

$$p(a_1^\tau, y_1^\tau) = \Pr(\mathbf{y}_1^\tau = y_1^\tau | a_1^\tau) \Pr(\mathbf{a}_1^\tau = a_1^\tau).$$

Since (min-log-BCJR approximation)

$$-\ln\left(\sum_k \exp(-\Delta_k)\right) \simeq \min_k \Delta_k \tag{10}$$

with Δ_k denoting nonnegative quantities, the exact log APP ratio $\lambda(\mathbf{a}_{n,j})$ is usually replaced by

$$\lambda(\mathbf{a}_{n,j}) \simeq \min_{\underline{a}_1^\tau, a_{n,j}=0} \{-\ln p(a_1^\tau, y_1^\tau)\} - \min_{\underline{a}_1^\tau, a_{n,j}=1} \{-\ln p(a_1^\tau, y_1^\tau)\} \tag{11}$$

where $\{-\ln p(a_1^\tau, y_1^\tau)\}$ is the cost metric of the trellis path associated with bit-labeled input sequence a_1^τ and received sequence y_1^τ. Due to trellis reduction, the SISO-DDFSE evaluates $\{-\ln p(a_1^\tau, y_1^\tau)\}$ in a suboptimal fashion based on per-survivor processing (PSP) [19]. For some given subtrellis $T(S, B)$, and some given particular branch metric, let $\mu_n^{\leftrightarrow}(b)$ be the cost metric of the best path starting from substate 0 at depth 0, terminating at substate 0 at depth τ (assuming tail symbols) and passing by branch $b \in B_n$ at section n. Suppose also that each branch $b \in B_n$ carries three fields: a departure substate $b^- \in S_{n-1}$, an arrival substate $b^+ \in S_n$, and a label $b^\blacktriangledown = \{b_1^\blacktriangledown, \ldots, b_q^\blacktriangledown\}$, modeling a bit-labeled input symbol for

the time-varying rate-1 convolutional ISI code at time instant n. The suboptimum SISO-DDFSE output can be written as

$$\lambda'(\mathbf{a}_{n,j}) = \min_{b\in B_n,\, b_j^{\blacktriangledown}=0} \mu_n^{\leftrightarrow}(b) - \min_{b\in B_n,\, b_j^{\blacktriangledown}=1} \mu_n^{\leftrightarrow}(b). \quad (12)$$

The path metric $\mu_n^{\leftrightarrow}(b)$, considered in (12) can always be split up into a sum of three terms

$$\mu_n^{\leftrightarrow}(b) = \mu_{n-1}^{\rightarrow}\left(b^-\right) + \xi_n(b) + \mu_n^{\leftarrow}\left(b^+\right) \quad (13)$$

where $\mu_n^{\rightarrow}(s)$, denoting the forward accumulated metric of the best subpath starting from substate $0 \in S_0$ and terminating in substate $s \in S_n$, is recursively computed according to

$$\mu_n^{\rightarrow}(s) = \min_{b\in B_{n-1},\, b^+=s} \left\{\mu_{n-1}^{\rightarrow}\left(b^-\right) + \xi_n(b)\right\} \quad (14)$$

with boundary conditions

$$\mu_0^{\rightarrow}(0) = 0 \quad \text{and} \quad \mu_0^{\rightarrow}(s) = \infty \qquad \forall\, s \neq 0 \quad (15)$$

where $\mu_n^{\leftarrow}(s)$, denoting the backward accumulated metric of the best subpath starting from substate $s \in S_n$ and terminating in substate $0 \in S_\tau$, is recursively computed according to

$$\mu_n^{\leftarrow}(s) = \min_{b\in B_{n+1},\, b^-=s} \left\{\mu_{n+1}^{\leftarrow}\left(b^+\right) + \xi_{n+1}(b)\right\} \quad (16)$$

with boundary conditions

$$\mu_\tau^{\rightarrow}(0) = 0 \quad \text{and} \quad \mu_\tau^{\rightarrow}(s) = \infty \qquad \forall\, s \neq 0. \quad (17)$$

The PSP-based branch metric $\xi_n(b)$ used by the SISO-DDFSE is expressed as

$$\xi_n(b) = \frac{1}{2\sigma^2}\left\| y_n - \hat{h}_0 z_n - \sum_{k=1}^{\nu_r} \hat{h}_k z_{n-k} - \sum_{k=\nu_r+1}^{\nu_c} \hat{h}_k \hat{z}_{n-k} \right\|^2 - \ln \Pr(\mathbf{b} = b) \quad (18)$$

and is calculated only once during the forward recursion and stored.

In the first term of (18), the complex symbol z_n entering the ISI code at time n results from simple remapping of the branch label $b^{\blacktriangledown,1}$. The complex symbol sequence $\{z_{n-\nu_r}, \ldots, z_{n-1}\}$ is simply deduced from substate b^-, whereas the estimated symbol sequence $\{\hat{z}_{n-\nu_c}, \ldots, \hat{z}_{n-\nu_r-1}\}$ is obtained by tracebacking the survivor path which terminates at b^- and by remapping labels on branches composing it. Survivor paths are supposed to be stored in a traceback sliding window of depth ν_c.

The log *a priori* probability $\ln \Pr(\mathbf{b} = b)$ on branch $b \in B_n$ in (18) can be formally identified to the log *a priori* probability on its carried label $b^{\blacktriangledown}$, so that

$$\ln \Pr(\mathbf{b} = b) = \ln \Pr(\mathbf{b}^{\blacktriangledown} = b^{\blacktriangledown}) = \ln \Pr\left(\underline{\mathbf{a}}_n = b^{\blacktriangledown}\right). \quad (19)$$

Assuming perfect decorrelation between log *a priori* probabilities on symbol bits $a_{n,j}$ after reinterleaving of log extrinsic probability ratio sequence coming from outer code C_o, we have

$$\ln \Pr(\mathbf{b} = b^{\blacktriangledown}) = \sum_{j=1}^{q} \ln \Pr\left(\mathbf{b}_j^{\blacktriangledown} = b_j^{\blacktriangledown}\right) = \sum_{j=1}^{q} \ln \Pr\left(\mathbf{a}_{n,j} = b_j^{\blacktriangledown}\right). \quad (20)$$

Finally, using (12), (13), and (20), the SISO-DDFSE output $\lambda'(\mathbf{a}_{n,j})$ on symbol bit $a_{n,j}$ can be split up into the sum of two logarithmic terms

$$\lambda'(\mathbf{a}_{n,j}) = \lambda_a(\mathbf{a}_{n,j}) + \lambda'_e(\mathbf{a}_{n,j}) \quad (21)$$

where

$$\lambda_a(\mathbf{a}_{n,j}) = \ln \frac{\Pr(\mathbf{a}_{n,j} = 1)}{\Pr(\mathbf{a}_{n,j} = 0)} \quad (22)$$

is the log *a priori* probability ratio on bit $a_{n,j}$ provided by outer decoding, and where

$$\lambda'_e(\mathbf{a}_{n,j}) = \min_{b\in B_n, b_j^{\blacktriangledown}=0} \left\{\mu_{n-1}^{\rightarrow}\left(b^-\right) + \xi_n^{e,j}(b) + \mu_n^{\leftarrow}\left(b^+\right)\right\} \quad (23)$$

$$- \min_{b\in B_n, b_j^{\blacktriangledown}=1} \left\{\mu_{n-1}^{\rightarrow}\left(b^-\right) + \xi_n^{e,j}(b) + \mu_n^{\leftarrow}\left(b^+\right)\right\} \quad (24)$$

with

$$\xi_n^{e,j}(b) = \frac{1}{2\sigma^2}\left\| y_n - \hat{h}_0 z_n - \sum_{k=1}^{\nu_r} \hat{h}_k z_{n-k} - \sum_{k=\nu_r+1}^{\nu_c} \hat{h}_k \hat{z}_{n-k} \right\|^2 - \sum_{\ell\neq j} \ln \Pr\left(\mathbf{a}_{n,\ell} = b_\ell^{\blacktriangledown}\right) \quad (25)$$

is the incremental knowledge (or log extrinsic probability ratio) on bit $a_{n,j}$ brought by all other bits of bit-labeled symbol of burst $\underline{a}_1^\tau$ throughout the ISI decoding process.

It must be emphasized that in case $\nu_r = \nu_c$, the SISO-DDFSE becomes formally equivalent to the min-log-BCJR algorithm applied on the full ISI channel trellis. When considering processing on a reduced-state trellis, estimated sequences taken from the path history and involved in branch metric derivations inevitably introduce a degradation in performance, due to a possible error propagation effect.

E. Minimum-Phase Prefiltering

If the main part of the ISI is contained in the last $\nu_c - \nu_r$ taps, the degradation in performance might be important compared to the min-log-BCJR ISI decoder. This happens when some roots of the equivalent discrete-time filter $H(z)$ are outside the unit circle. To assure an average error rate close to optimal performance, a correcting-phase prefiltering must be fitted just before the SISO-DDFSE. This prefilter turns the discrete-time channel impulse response into minimum phase, concentrating energy in the first taps, thus improving the accuracy of DDFSE branch

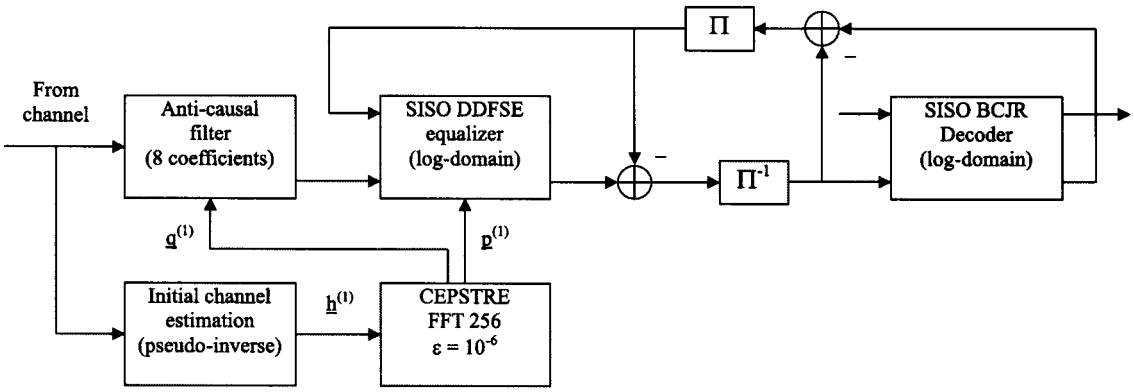

Fig. 6. A low-complexity turbo-detector.

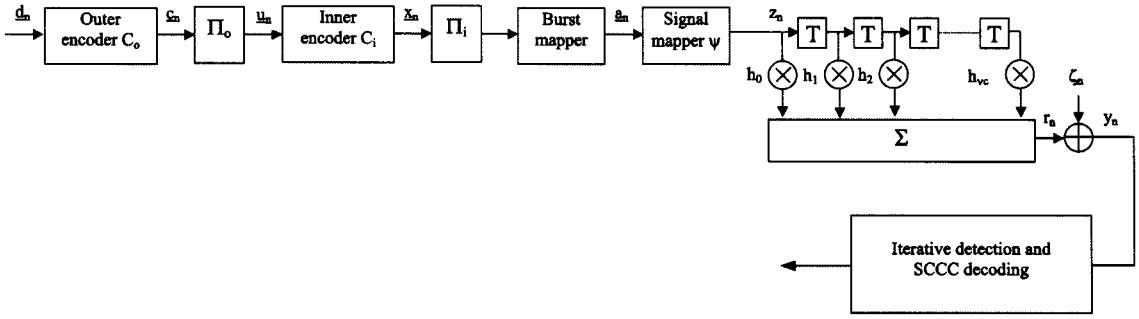

Fig. 7. Equivalent discrete-time model of scheme 2.

metrics dramatically. Many algorithms exist to practically construct the minimum-phase filter, the most straightforward being based on root finding. Because of its prohibitive complexity, however, the CEPSTRE principle has been preferred here for an efficient calculation [20]. A low-complexity turbo detector is depicted on Fig. 6.

III. Iterative Detection and SCCC Decoding

A. Equivalent Discrete-Time Model

In this new scheme (scheme 2), a data sequence $\underline{d}_1^{\tau_o} = \{\underline{d}_1, \ldots, \underline{d}_{\tau_o}\}$ is first encoded by an outer channel encoder C_o, which generates an outer coded sequence $\underline{c}_1^{\tau_o} = \{\underline{c}_1, \ldots, \underline{c}_{\tau_o}\}$. Each data symbol $\underline{d}_n = [d_{n,1}, d_{n,2}, \ldots, d_{n,k_o}]$ contains k_o bits, whereas each coded symbol $\underline{c}_n = [c_{n,1}, c_{n,2}, \ldots, c_{n,n_o}]$ contains n_o bits. Coded bits are interleaved by a pseudo-random interleaver Π_o. The interleaved sequence $\underline{u}_1^{\tau_i} = \{\underline{u}_1, \ldots, \underline{u}_{\tau_i}\}$, with $\underline{u}_n = [u_{n,1}, u_{n,2}, \ldots, u_{n,k_i}]$ containing k_i bits, enters an inner channel code C_i. The produced coded sequence $\underline{x}_1^{\tau_i} = \{\underline{x}_1, \ldots, \underline{x}_{\tau_i}\}$, with $\underline{x}_n = [x_{n,1}, x_{n,2}, \ldots, x_{n,n_i}]$ containing n_i bits is interleaved by a pseudo-random channel interleaver Π_i and divided into N bursts $\underline{a}_1^{\tau} = \{\underline{a}_1, \ldots, \underline{a}_{\tau}\}$ of τ bit-labeled symbols (including known symbols for channel estimation and synchronization purposes). To each symbol $\underline{a}_n = [a_{n,1}, a_{n,2}, \ldots, a_{n,q_i}]$ on $q_i = \log_2 Q_i$ bits, a Q_i-ary signal mapper Ψ associates a complex-valued symbol z_n. We represent in Fig. 7 the corresponding equivalent discrete-time model of scheme 2. Scheme 2 is spectrally equivalent to scheme 1 if the inner coding rate $\rho_i = k_i/n_i$ is compensated by an increase of the modulation order Q_i compared to Q. In other words, equivalence is assured if $Q_i/Q = 2^{n_i - k_i}$.

B. Iterative Decoding

Modulation order increase usually makes an optimal symbol-by-symbol detection unrealistic for scheme 2. Hence, we have no option other than using a suboptimal SISO-DDFSE to perform the detection task. On the other hand, the serially concatenated codes C_o and C_i will be optimally decoded by employing a log-BCJR algorithm at both stages. At first iteration, for each burst, the SISO-DDFSE computes a log extrinsic ratio $\lambda_e'(\mathbf{a}_{n,j})$ on each bit of each symbol $\underline{a}_n$, given the complex valued received burst y_1^{τ} and a channel estimate (or reestimate) vector $\underline{\hat{h}}$. The N sequences of log *a priori* probability ratios on symbol bits $a_{n,j}$ is set to 0. After channel deinterleaving Π_i^{-1}, the overall sequence of log extrinsic ratios is used by an inner SISO decoder as a sequence of log *intrinsic* probability ratios on inner coded bits $x_{n,j}$. The inner SISO decoder first computes a log extrinsic ratio $\lambda_e(\mathbf{u}_{n,j})$ on each inner data bit $u_{n,j}$. The produced sequence is deinterleaved by Π_o^{-1} and passed to an outer decoder as a sequence of log *a priori* probability ratios on outer coded bits $c_{n,j}$. The inner SISO decoder also computes log extrinsic probability ratios $\lambda_e(\mathbf{x}_{n,j})$ on each inner coded bit $x_{n,j}$. The produced sequence is reinterleaved by Π_i and sent to the SISO-DDFSE as N sequences (one per burst) of log *a priori* probability ratios on symbol bits $a_{n,j}$ for the next iteration. To complete this first iteration, the outer SISO decoder finally computes a log extrinsic ratio $\lambda_e(\mathbf{c}_{n,j})$ on each outer coded bit $c_{n,j}$. The produced sequence is reinterleaved by Π_o and passed to the inner SISO decoder as a sequence of log *a priori* probability ratios on inner

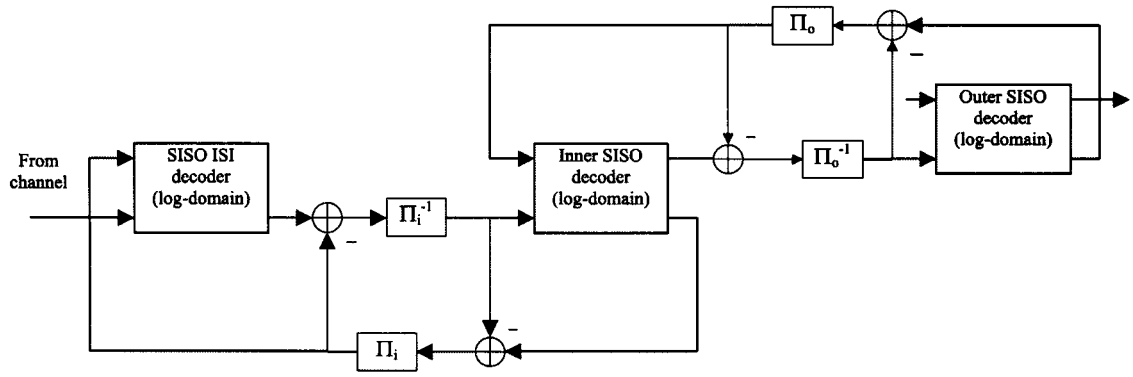

Fig. 8. Iterative decoding of scheme 2.

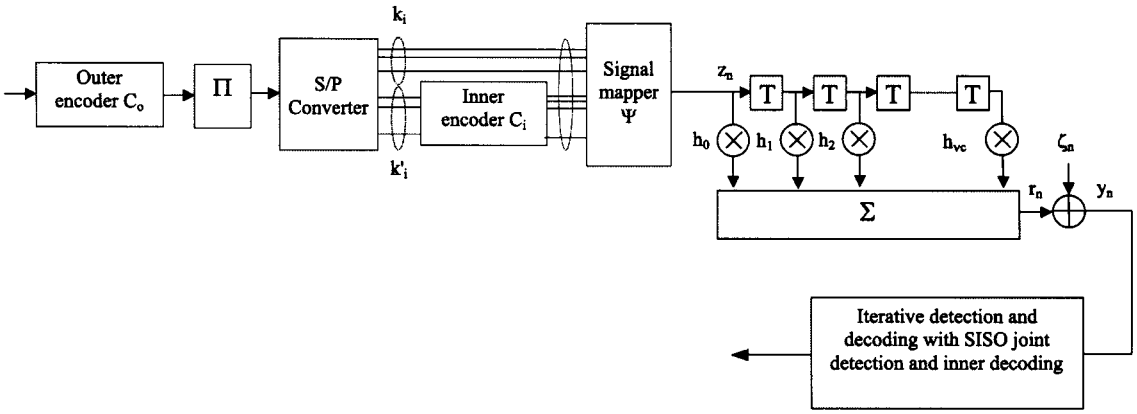

Fig. 9. Equivalent discrete-time model of scheme 3.

data bits $u_{n,j}$ for the next iteration. A recapitulative diagram of the iterative decoding process is shown in Fig. 8.

IV. Iterative Detection and Decoding of Serially Concatenated TCM

A. Equivalent Discrete-Time Markovian Model of Inner Part and Associated Possibly Reduced Trellis

Fig. 9 illustrates the equivalent discrete-time model associated with a third scheme (scheme 3), where we consider an outer code C_o concatenated with a TCM Ξ_i, followed by an ISI code. The Π-interleaved outer encoded sequence is divided into N data bursts $\underline{u}_1^\tau = \{\underline{u}_1, \underline{u}_2, \ldots, \underline{u}_\tau\}$ of τ bit-labeled symbols, each data symbol $\underline{u}_n = [u_{n,1}, u_{n,2}, \ldots, u_{n,k_i}]$ containing k_i bits. The inner TCM Ξ_i, of rate ρ_i, operates on $k_i' \leq k_i$ input bits and produces N coded bursts $\underline{x}_1^\tau = \{\underline{x}_1, \underline{x}_2, \ldots, \underline{x}_\tau\}$ where each symbol $\underline{x}_n$ contains $n_i = (k_i'/\rho_i)+(k_i-k_i')$ coded and encoded bits $[x_{n,1}, x_{n,2}, \ldots, x_{n,n_i}]$. To any coded symbol $\underline{x}_n$, the nonlinear TCM mapping rule Ψ associates a Q_i-ary complex valued symbol z_n. Again, scheme 3 is spectrally equivalent to scheme 1 $Q_i/Q = 2^{((1/\rho_i)-1)k_i}$. The combination of TCM and ISI channel encoding can be regarded as a Markovian process whose memory is the sum of the memories of the constituents and which accepts a "super-trellis" diagram $T(S, B)$ as a graphical representation. If, for convenience, we suppose that the TCM encoder is a time-invariant nonrecursive convolutional code of memory ν_i, the super-trellis is regular, made of one single section $T_n(S_n, B_n)$, which is repeated in time. The combined states can be expressed in terms of the inner data sequence as $s_n = \{\underline{u}_{n-\nu_i-\nu_c}, \ldots, \underline{u}_{n-1}\}$ so that super-trellis complexities are given by

$$|S_n| = 2^{(\nu_i+\nu_c)k_i}, \qquad \forall n \in [0, \tau]$$

and

$$|B_n| = 2^{(\nu_i+\nu_c+1)k_i}, \qquad \forall n \in [1, \tau]. \tag{26}$$

B. SISO Joint Detection and TCM Inner Decoding

At each section $n \in [1, \tau]$ and for all inner data bit indexes $j \in [1, k_i]$, an optimal symbol-by-symbol algorithm would compute the log APP ratio, defined as

$$\lambda(\mathbf{u}_{n,j}) = \ln \frac{\Pr\left(\mathbf{u}_{n,j} = 1 \middle| y_1^\tau, \hat{\underline{h}}\right)}{\Pr\left(\mathbf{u}_{n,j} = 0 \middle| y_1^\tau, \hat{\underline{h}}\right)}. \tag{27}$$

As previously stated, such a ratio could be optimally computed by the BCJR algorithm processing on the full combined ISI and TCM super-trellis. The decoding complexity would be so high, however, that such an optimal approach must be discarded and replaced by suboptimal ones operating on reduced-state trellises. Again, for a positive integer ν_r, we say that a trellis inner input sequence $\underline{u}_1^n$ ends at substate s if $\underline{u}_1^n$ terminates with the substring $s = \underline{u}_{n-\nu_r+1}^n$. The substate space S_n at any depth n coincides with the super-trellis state space S_n if $\nu_r = \nu_c + \nu_i$. In the case where $\nu_r < \nu_c + \nu_i$, S_n is reduced to the subset of

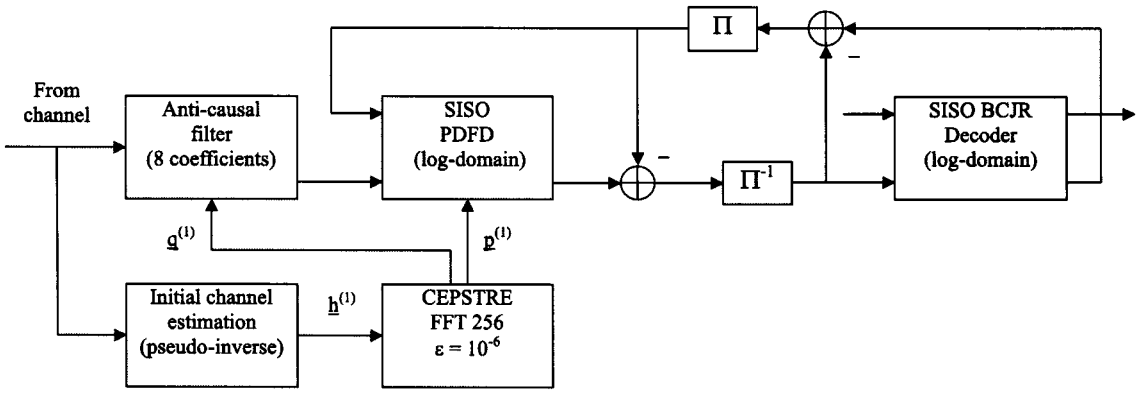

Fig. 10. Iterative decoding of scheme 3.

S_n made of all possible substates s derived from full states s, whose complexity is

$$|S_n| = 2^{\nu_r k_i}, \qquad \forall\, n \in [0, \tau]. \tag{28}$$

Without loss of generality, let us focus on the special subcase where ν_r is chosen equal to ν_i. Path metrics computation and minimization are then directly performed on the regular TCM trellis $T(S, B)$. The resulting suboptimal SISO algorithm is called SISO parallel decision-feedback decoder (or SISO-PDFD). Carrying out a similar forward–backward derivation as was done for SISO-DDFSE, the final SISO-PDFD output

$$\lambda'(\mathbf{u}_{n,j}) = \lambda_a(\mathbf{u}_{n,j}) + \lambda'_e(\mathbf{u}_{n,j}) \tag{29}$$

is equivalently obtained by just modifying the branch metric for existing transitions

$$\xi_n(b) = \frac{1}{2\sigma^2}\left\| y_n - \hat{h}_0 z_n - \sum_{k=1}^{v_c} \hat{h}_k \hat{z}_{n-k} \right\|^2 - \ln \Pr(\mathbf{b} = b). \tag{30}$$

In the first term of (30), the complex symbol z_n results from simple remapping of the branch label $b^{\blacktriangledown,2}$, which, in this new case, models the bit-labeled coded symbol produced by the TCM for transition b (the first one $b^{\blacktriangledown,1}$ is used in $\lambda'(\mathbf{u}_{n,j})$ computation modeling the bit-labeled input entering the TCM for transition b). The estimated symbol sequence $\{\hat{z}_{n-\nu_r}, \ldots, \hat{z}_{n-1}\}$ is obtained by tracebacking the survivor path which terminates at b^- and by remapping labels on branches composing it. Survivor paths are supposed to be stored in a traceback sliding window of depth ν_c.

The fundamental interest of the SISO-PDFD lies in the fact that the ISI introduced by the channel is not taken into account any more in trellis substates. Its complexity is linear in $|B|$ and does not depend either on modulation order Q_i or on ISI code memory ν_c. However, since ISI contribution is estimated using past symbols read on stored survivors, the SISO-PDFD inherently suffers from error propagation effect, especially when a significant part of the energy is concentrated in middle and last taps. Hence, as for the SISO-DDFSE, a prefiltering is crucially needed to turn the channel into minimum phase, before performing joint detection and decoding.

C. Iterative Decoding

At first iteration, for each burst, the SISO-PDFD suboptimally computes a log extrinsic ratio $\lambda'_e(\mathbf{u}_{n,j})$ on each inner coded bit, given the complex valued received burst y_1^T and an channel estimate (or reestimate) vector $\underline{\hat{h}}$ of the equivalent discrete-time channel coefficients. No log *a priori* information is yet available on bits $u_{n,j}$. The produced sequences are deinterleaved by Π^{-1} and sent to the outer SISO decoder as a sequence of log *intrinsic* probability ratio on outer coded bits $c_{n,j}$. The outer SISO decoder then computes a log extrinsic probability ratio $\lambda_e(\mathbf{c}_{n,j})$ on each outer coded bit $c_{n,j}$. The produced sequence is reinterleaved by Π and passed to the SISO-PDFD as N sequences (one per burst) of log *a priori* probability ratios on inner data bits $u_{n,j}$ for a next joint detection and inner decoding attempt. A recapitulative diagram is depicted in Fig. 10.

V. Schemes Comparison in Terms of Performance

To evaluate and compare the proposed schemes (1, 2, and 3) in terms of performance, simulations have been realized on a static ISI channel with five independent paths. The attenuation factors of all paths have been chosen as

$$\underline{h} = \left[\sqrt{0,45}\ \sqrt{0,25}\ \sqrt{0,15}\ \sqrt{0,1}\ \sqrt{0,05}\right]$$

so that the total mean power is normalized to 1. Such a minimum-phase channel creates an ISI theoretical loss of approximately 3.0 dB.

For inner and outer codes of scheme 2 and outer code of scheme 3, we have used four-state recursive systematic convolutional (RSC) codes of rate $1/2$ and generator polynomes $(1, (1+D^2/(1+D+D^2))$. In scheme 2, whose performance is shown on Fig. 11 with optimal ISI decoding, SCCC interleaver depth has been chosen equal to $N_o = 2048$ bits (leading to a channel interleaver depth of $N_i = 4096$ bits) and the modulation is QPSK. In scheme 3, whose performance is plotted on Fig. 12, the TCM is made of a four-state nonrecursive nonsystematic convolutional (NRNSC) code of rate $1/2$ and generator polynomes $(1 + D^2, 1 + D + D^2)$, coupled with Gray mapping. As a benchmark, we have also simulated the conventional turbo detection scheme 1, made of one single RSC code of rate $1/2$ and generator polynomes $(1, (1 + D^2/1 + D + D^2))$. For scheme 1A (Fig. 13), an optimal ISI decoding is realized, whereas scheme 1B (Fig. 14) employs a SISO-DDFSE with

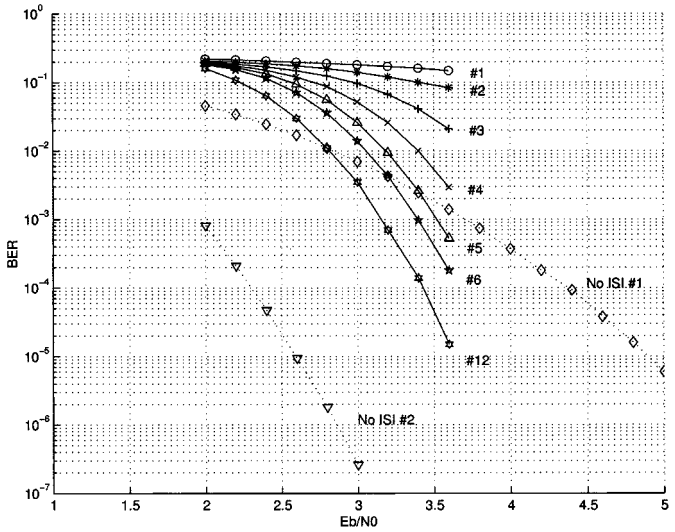

Fig. 11. Scheme 2A—Iterative decoding of SCCC concatenated with ISI code (rate 1/2 four-state RSC inner code, rate 1/2 four-state RSC outer code, QPSK, five-tap min-phase static channel, Log-BCJR ISI decoder).

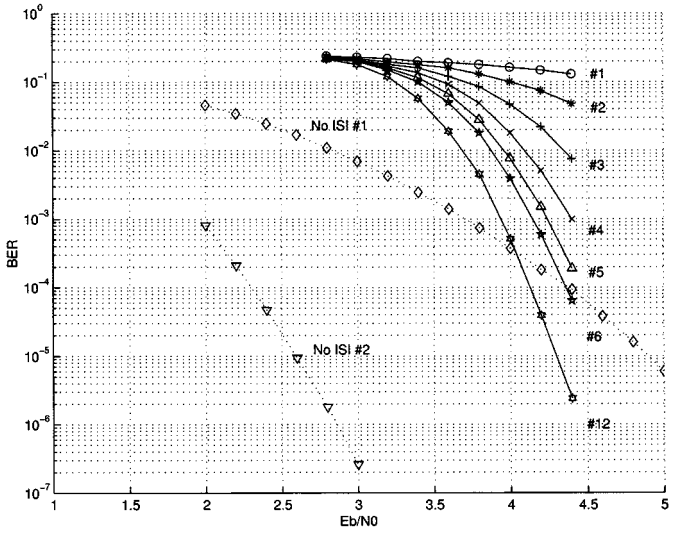

Fig. 12. Scheme 3—Iterative decoding of outer code concatenated with TCM using PDFD (rate 1/2 four-state RSC outer code, rate 1/2 four-state NRNSC inner code + QPSK, five tap min phase static channel).

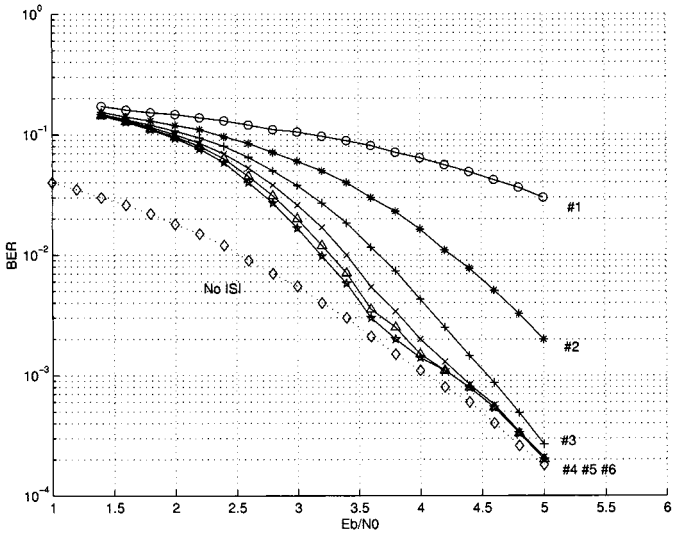

Fig. 13. Scheme 1A—Turbo decoder using Log-BCJR ISI decoder (rate 1/2 four-state RSC outer code, BPSK, five tap min phase static channel).

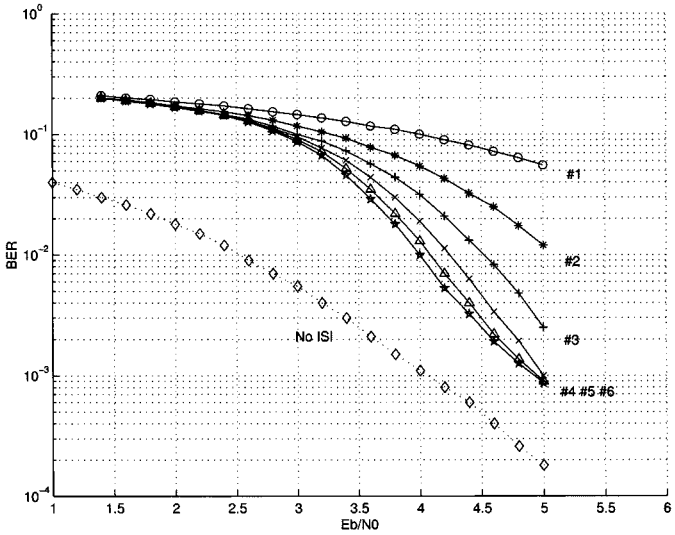

Fig. 14. Scheme 1B—Low-complexity turbo-decoder using SISO-DDFSE $\nu_r = 2$ (rate 1/2 four-state RSC outer code, BPSK, five tap min phase static channel).

$\nu_r = 2$ which leads to a degradation of 1 dB at BER $= 10^{-3}$. If a BPSK modulation is assumed together with a channel interleaver depth of $N = 2048$ bits, such a reference scheme has in fact the same spectral occupation than others. At reception, the channel is supposed to be known in all cases.

Observation of Figs. 11–13 reveals that scheme 2 provides the best performance, which is only 0.7 dB better than the performance of scheme 3. Iterative process for scheme 2 also starts 1 dB earlier than others. Its computational complexity is, however, exorbitant. If suboptimum SISO-DDFSE is used in scheme 2 (Fig. 15), a reduction factor of 16 is reached with $\nu_r = 2$, but the corresponding performance loss of 2.0 dB makes this scenario not so attractive in practice. The great advantage of scheme 3 lies in its computational complexity 128 times less than scheme 2 (with optimal ISI decoding), for an almost similar performance (neglecting the prefiltering and PSP complexity).

Fig. 13 also shows that the "no_ISI" curve corresponding to the optimal decoding performance of a RSC code on a Gaussian channel and acting as the theoretical lower bound for scheme 1A (optimal ISI decoding) is clearly outperformed by schemes 2 and 3. As expected, this is due to the more powerful code combination involved in the last two. It must also be emphasized that computational complexity of the 12 iterations of scheme 3 is of the same order as five iterations of scheme 1A, for a far better asymptotic performance of the former. (Note that we did not take into account the additional complexity due to PSP.)

From this analysis, we conclude that scheme 3 provides the best compromise between performance and complexity. Unfortunately, it cannot be applied for highly frequency selective channels. Indeed, for most channel outcomes, the prefiltering reveals powerless to fight against the error propagation that appears in SISO-PDFD branch metrics computation. As a consequence, a new generalized SISO-PDFD has been investigated

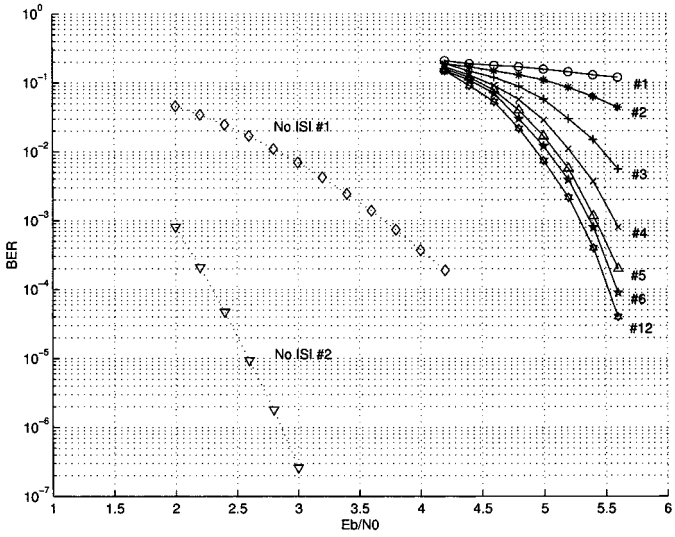

Fig. 15. Scheme 2B—Iterative decoding of SCCC concatenated with ISI code (rate 1/2 four-state RSC inner code, rate 1/2 four-state RSC outer code, QPSK, five-tap min-phase static channel, SISO-DDFSE $\nu_r = 2$).

in [24] and [25], which is proved to be very efficient against this per-survivor processing limitation.

VI. Turbo Detection Combined With Channel Reestimation

A. EM Based Reestimation

As mentioned previously, the SISO ISI decoders presented in Sections II and III and simulation results presented above assume that the channel coefficient vector $\underline{h} = [h_0, \ldots, h_{\nu_c}]$ is known at the receiver. In practice, channel coefficients are estimated by inserting a known constant amplitude zero autocorrelation (CAZAC) training sequence in the transmitted frame at the expense of reduced spectral efficiency. The classical method of correlative channel estimation (the pseudo-inverse method) causes a performance degradation of 2.9 dB with respect to the perfect channel estimation [26]. This gap can be reduced by using more advanced channel estimation techniques, such as the expectation-maximization (EM) algorithm, a powerful tool that performs maximum likelihood (ML) parameter estimation of a doubly stochastic process in an iterative fashion [27]. The EM channel estimation of this work utilizes the decoupling decomposition proposed in [28] together with the forward–backward trellis search of the SISO ISI decoder to obtain separate closed form recursion expressions for channel coefficient estimates.

The optimum ML solution to the problem of channel estimation $\underline{\hat{h}}_{\mathrm{ML}}$ is obtained by maximizing the log likelihood function of the received vector of samples

$$\underline{\hat{h}}_{\mathrm{ML}} = \arg\max_{\underline{h}} \log p\left(y_1^{\tau} \left| \underline{h}\right.\right). \tag{31}$$

In most cases, finding the solution of (31) is practically impossible. However, the EM algorithm provides a feasible solution to this optimization problem by iteratively reestimating the channel coefficients, so that a monotonic increase in the likelihood function is guaranteed. It achieves this monotonic increase by introducing the following auxiliary function:

$$Q\left(\underline{h} \left| \underline{\hat{h}}^{(\iota)}\right.\right) = E_{\mathbf{w}}\left\{\log p\left(\mathbf{w}|\underline{h}\right) \left| y_1^{\tau}, \underline{\hat{h}}^{(\iota)}\right.\right\} \tag{32}$$

where $\underline{\hat{h}}^{(\iota)}$ is the vector of estimated channel coefficients at the ιth iteration of turbo-detector and $\mathbf{w}$ is the so-called *complete data* that is actually unobservable, but whose knowledge makes the estimation easy. Since the complete data $\mathbf{w}$ is unknown, its log-likelihood function is a random variable, and therefore we maximize the conditional mean of this log-likelihood function given the (observable) *incomplete data* y_1^{τ} and the set of most recent channel estimates $\underline{\hat{h}}^{(\iota)}$. The complexity and the rate of convergence of the algorithm is affected by the choice of the complete data $\mathbf{w}$.

As depicted in Fig. 16, the EM reestimation sequencing is as follows: during each iteration ι of the turbo detector, an iteration of the EM algorithm is performed together with the SISO equalization process. This EM iteration itself involves a two-step procedure:

1) E-step: Compute

$$Q\left(\underline{h} \left| \underline{\hat{h}}^{(\iota)}\right.\right) = E_{\mathbf{w}}\left\{\log p\left(\mathbf{w}|\underline{h}\right) \left| y_1^{\tau}, \underline{\hat{h}}^{(\iota)}\right.\right\};$$

2) M-step: Solve

$$\underline{\hat{h}}^{(\iota+1)} = \arg\max_{\underline{h}} Q\left(\underline{h} \left| \underline{\hat{h}}^{(\iota)}\right.\right).$$

The new vector of channel coefficients $\underline{\hat{h}}^{(\iota+1)}$ is used by the SISO ISI decoder at iteration $\iota + 1$ of the turbo detector. The expectation operation in the E-step is with respect to the complete data $\mathbf{w}$. The performance of the EM algorithm is very sensitive to the choice of the initial estimate $\underline{\hat{h}}^{(0)}$. Therefore, we initialize the algorithm by applying the pseudo-inverse method on the training sequence.

It has been shown in [28] that for the class of problems involving superimposed signals, there is a natural choice of complete data, leading to simple analytical expressions to extract the ML estimates. This is achieved by decomposing the noise components ζ_n (that are present in the received samples) arbitrarily (and artificially) into independent noise processes $\zeta_{n,0}, \ldots, \zeta_{n,\nu_c}$ whose number is equal to the number $\nu_c + 1$ of superimposed signals. Adopting this approach, and considering that our problem also includes the unknown transmitted symbols as random parameters, we choose the complete data as $\mathbf{w} = (\underline{\underline{\mathbf{\Theta}}}, \mathbf{z}_1^{\tau})$where $\mathbf{z}_1^{\tau} = \{\mathbf{z}_1, \mathbf{z}_2, \ldots, \mathbf{z}_{\tau}\}$ is the random sequence composed of the complex transmitted symbols and $\underline{\underline{\mathbf{\Theta}}}$ is chosen as a random matrix whose (n, k)th entry is given by a process formed by adding one of the superimposed signals and its corresponding noise component

$$\theta_{n,k} = \mathbf{h}_k \mathbf{z}_{n-k} + \zeta_{n,k} \tag{33}$$

and $\{\zeta_{n,0}, \ldots, \zeta_{n,\nu_c}\}$ is the set of noise components that are complex, independent, and identically distributed (i.i.d.), zero-mean Gaussian random variables with variances $\sigma_k^2 = E\{|\zeta_{n,k}|^2\} = \varsigma_k N_0$. Clearly, ς_ks have to satisfy the normalization constraint $\sum_{k=0}^{\nu_c} \varsigma_k = 1$. Besides, it is stated

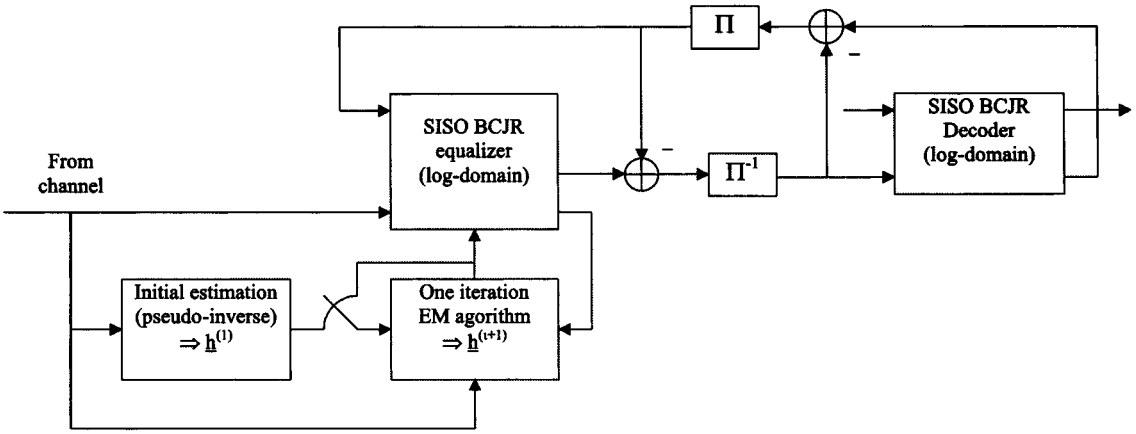

Fig. 16. EM channel reestimation.

in that introducing variations in the choice of the ς_ks can be helpful to control the rate of convergence of the EM algorithm and to avoid the convergence to an unwanted stationary point. In our simulations, however, we have taken $\varsigma_k = 1/(\nu_c + 1)$ for all k.

Having defined the complete data $\mathbf{w}$, we can write the objective function as follows (see the Appendix):

$$\begin{aligned} Q\left(\underline{h}\left|\underline{\hat{h}}^{(\iota)}\right.\right) &= \frac{2}{N_0}\sum_{k=0}^{\nu_c}\frac{1}{\varsigma_k}\sum_{n=1}^{\tau} \cdot \Re e\left\{h_k^* \sum_{s\in \mathrm{A}^{\nu_c+1}} s_k^* \overline{\theta}_{n,k} \Pr\left(\mathbf{z}_{n-\nu_c}^n = s \left| y_1^\tau, \underline{\hat{h}}^{(\iota)}\right.\right)\right\} \\ &\quad - \frac{1}{N_0}\sum_{k=0}^{\nu_c}\frac{1}{\varsigma_k}\sum_{n=1}^{\tau}|h_k|^2 \sum_{s\in \mathrm{A}^{\nu_c+1}}|s_k|^2 \cdot \Pr\left(\mathbf{z}_{n-\nu_c}^n = s \left| y_1^\tau, \underline{\hat{h}}^{(\iota)}\right.\right) \end{aligned} \tag{34}$$

where $*$ denotes the complex conjugate operator, A denotes the modulation alphabet, $\mathbf{z}_{n-\nu_c}^n$ denotes the (complex-valued equivalent) EM algorithm state at time n, s is some possible realization in A^{ν_c+1} whose kth component is s_k, and

$$\overline{\theta}_{n,k} = \int_{\theta_{n,k}} \theta_{n,k} p\left(\theta_{n,k}\left| s, y_1^\tau, \underline{\hat{h}}^{(\iota)}\right.\right) d\theta_{n,k} \tag{35}$$

is the conditional expectation of $\theta_{n,k}$ given $(s, y_1^\tau, \underline{\hat{h}}^{(\iota)})$. For phase modulated systems, the second term of $Q(\underline{h}|\underline{\hat{h}}^{(\iota)})$ in (34) reduces to $-(1/2)|h_n|^2\varepsilon$ where ε is the energy of the symbols.

The essence of the decomposition in defining the complete data $\mathbf{w}$ can be clearly seen in the expression of the objective function. The complicated superimposed parameter optimization problem which leads to nonlinear expressions is decoupled into ν_c+1 separate ML optimizations leading to tractable linear expressions.

The M-step is performed by taking the partial derivative of $Q(\underline{h}|\underline{\hat{h}}^{(\iota)})$ with respect to each channel coefficient h_k and equating the resulting expressions to zero to extract $\hat{h}_k^{(\iota+1)}$ for all k. Then, we obtain the recursive expression to update the channel coefficient estimates as follows:

$$\hat{h}_k^{(\iota+1)} = \frac{\sum_{n=1}^{\tau}\sum_{s\in \mathrm{A}^{\nu_c+1}} s_k^* \overline{\theta}_{n,k} \Pr\left(\mathbf{z}_{n-\nu_c}^n = s \left| y_1^\tau, \underline{\hat{h}}^{(\iota)}\right.\right)}{\sum_{n=1}^{\tau}\sum_{s\in \mathrm{A}^{\nu_c+1}} |s_k|^2 \Pr\left(\mathbf{z}_{n-\nu_c}^n = s \left| y_1^\tau, \underline{\hat{h}}^{(\iota)}\right.\right)} \tag{36}$$

with

$$\overline{\theta}_{n,k} = \hat{h}_k^{(\iota)} s_k + \varsigma_k\left[y_n - \sum_{m=0}^{\nu_r-1}\hat{h}_m^{(\iota)} s_m\right]. \tag{37}$$

Due to the ISI Markovian structure, the *a posteriori* conditional probabilities $\Pr(\mathbf{z}_{n-\nu_c}^n = s|y_1^\tau, \underline{\hat{h}}^{(\iota)})$ can easily be obtained from the forward–backward recursion trellis search performed by the ISI SISO decoder. Thus, the EM channel reestimation can be naturally embedded in the iterative detection process without bringing a significant overhead. For an optimal BCJR detection, and following the formalism of [10], we can explicitly compute the EM algorithm state APPs by

$$\begin{aligned} &\Pr\left(\mathbf{z}_{n-\nu_c}^n = s \left| y_1^\tau, \underline{\hat{h}}^{(\iota)}\right.\right) \\ &= \frac{p\left(\mathbf{z}_{n-\nu_c+1}^n = s, y_1^\tau \left| \underline{\hat{h}}^{(\iota)}\right.\right)}{\sum_{s'\in S_n} p\left(\mathbf{z}_{n-\nu_c+1}^n = s', y_1^\tau \left| \underline{\hat{h}}^{(\iota)}\right.\right)} \end{aligned} \tag{38}$$

where the joint probability $p(\mathbf{z}_{n-\nu_c+1}^n = s', y_1^\tau|\underline{\hat{h}}^{(\iota)})$ can be split into

$$p\left(\mathbf{z}_{n-\nu_c+1}^n = s', y_1^\tau \left| \underline{\hat{h}}^{(\iota)}\right.\right) = \alpha_n(s')\beta_n(s') \tag{39}$$

with

$$\alpha_n(s') = p\left(\mathbf{z}_{n-\nu_c+1}^n = s', y_1^n \left| \underline{\hat{h}}^{(\iota)}\right.\right) \tag{40}$$

and

$$\beta_n(s') = p\left(y_{n+1}^\tau \left| \mathbf{z}_{n-\nu_c+1}^n = s', \underline{\hat{h}}^{(\iota)}\right.\right). \tag{41}$$

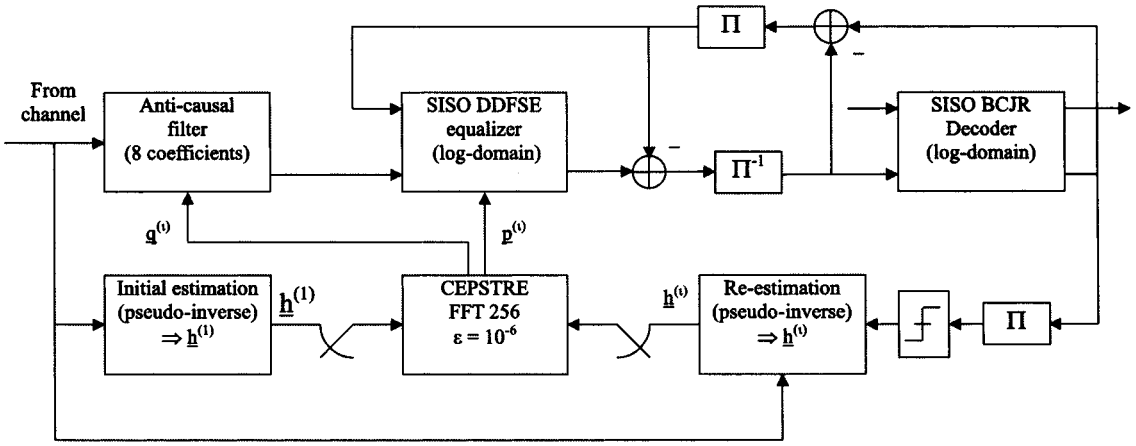

Fig. 17. Bootstrap channel reestimation.

B. A Simple Suboptimal Linear Alternative for the Channel Reestimation Problem

This very simple approach is inspired by the well-known bootstrap technique. Instead of considering estimated data symbols after the ISI decoder, however, decisions are taken after reinterleaving of the decoded sequence $\underline{c}_1^\tau$. Thus, the so-called bootstrap reestimation benefits from time diversity brought by interleaving and from channel decoding efficiency.

We now describe the sequencing.

1) After Π reinterleaving of soft outputs on $\underline{c}_1^\tau$ produced by the channel decoder, a hard decision is taken on each bit $a_{n,j}$ of each bit-labeled symbol $\underline{a}_n$ of sequence $\underline{a}_1^\tau$. An estimate of useful symbols, denoted $\hat{\underline{a}}_1^{\tau(\iota)}$, is then available (tail symbols, guard symbols, and symbols of CAZAC training sequence are known *a priori*).
2) The matrix system is formed by

$$y_1^\tau = \underline{\underline{A}}^{(\iota)} \underline{h} + \zeta_1^\tau \tag{42}$$

where

y_1^τ sequence of observed symbols;
$\underline{h}$ unknown vector of channel coefficients;
$\underline{\underline{A}}^{(\iota)}$ Toeplitz square matrix whose complex coefficients are made of estimated symbols of $\hat{\underline{a}}_1^{\tau(\iota)}$ at iteration ι.

3) A solution minimizing the error probability (or, equivalently, the Euclidean distance, ζ_1^τ being a Gaussian random vector with circular symmetry) is well-known

$$\hat{\underline{h}}^{(\iota+1)} = \left[\left(\underline{\underline{A}}^{(\iota)}\right)^* \underline{\underline{A}}^{(\iota)}\right]^{-1} \left(\underline{\underline{A}}^{(\iota)}\right)^* y_1^\tau \tag{43}$$

where $*$ denotes transpose conjugate operator. Matrix system (43) can be solved by a Choleski decomposition. Exhibited $\hat{\underline{h}}^{(\iota+1)}$ is used as a channel estimate for iteration $\iota+1$.

A recapituative diagram is shown in Fig. 17 for the full turbo DDFSE-based receiver.

C. Performance Analysis

Fig. 18 depicts the simulation results on the raw BER performance of the classical turbo detection scheme (optimal BCJR-based ISI decoding) that uses a 16-state RSC code of rate 1/2 and generator polynomials $(1, (1+D+D^2+D^4)/(1+D+D^4))$ on the static five-tap minimum-phase channel

$$\underline{h} = \left[\sqrt{0.45}\,\sqrt{0.25}\,\sqrt{0.15}\,\sqrt{0.1}\,\sqrt{0.05}\right]$$

with EM channel reestimation. For comparison purposes, the corresponding performances of the perfect channel estimation and the classical pseudo-inverse channel estimation with 26-symbol CAZAC training sequence are also included in the same figure. The pseudo-inverse channel estimation is done only at the beginning of the turbo iterations and is not updated within the course of the turbo iterations. The initial estimate for the EM reestimation is obtained with the pseudo-inverse method.

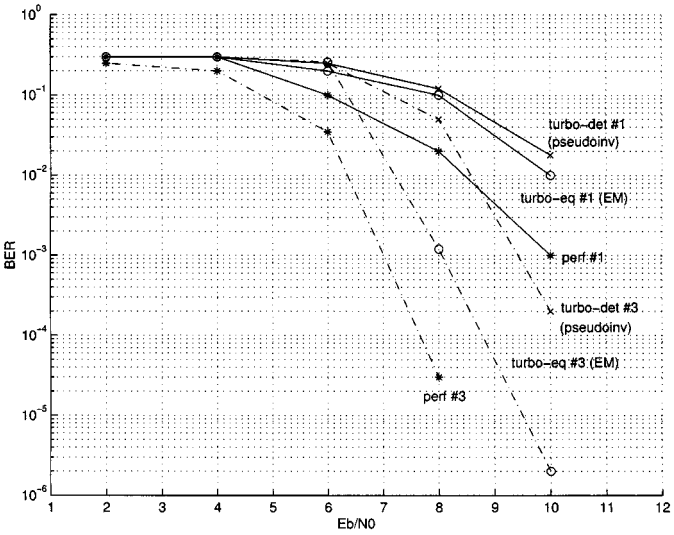

Fig. 18. Scheme 1A—Full turbo detector (rate 1/2 16-state RSC outer code, BPSK, five-tap min phase static channel) with log-BCJR ISI decoder and EM channel reestimation.

It can be observed that even with a single EM iteration, the performance of the EM-based channel reestimation outperforms the classical pseudo-inverse channel estimation by 1.5 dB and is inferior with respect to the perfect channel estimation by 1 dB. Furthermore, the effect of updating the channel coefficient estimates at each turbo iteration can clearly be observed, i.e., the

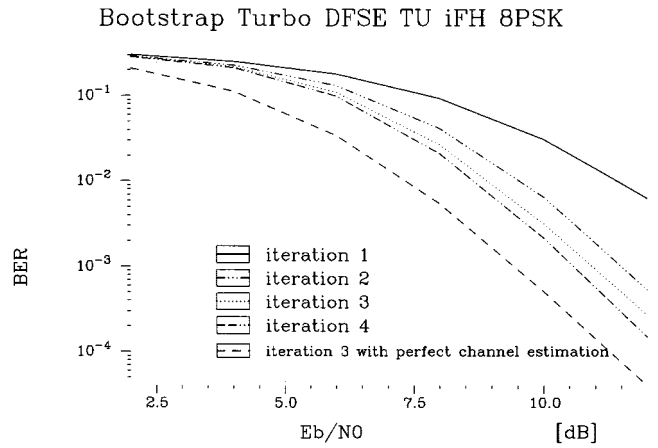

Fig. 19. Scheme 1B—Low-complexity full turbo-detector (rate 1/2 16-state RSC outer code, eight-PSK, TU channel profile) with SISO-DDFSE ($\nu_r = 2$) and bootstrap channel reestimation.

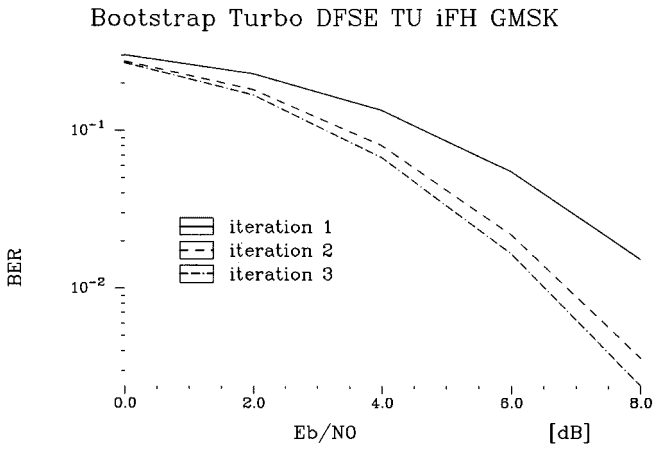

Fig. 20. Scheme 1B—Low-complexity full turbo-detector (rate 1/2 16-state RSC outer code, GMSK, TU channel profile) with SISO-DDFSE ($\nu_r = 5$) and bootstrap channel reestimation.

superiority of the EM channel reestimation over the pseudo-inverse method increases with the turbo iteration index. In iteration 1, the difference is less than 0.5 dB, whereas in iteration 3, it is approximately 1.5 dB.

Figs. 19 and 20 show simulation results for a time-varying and frequency-selective GSM typical urban (TU) channel at low speed (the channel is assumed to be stationary over the duration of each radio burst defined as in [18]) and ideal frequency hopping (the channel is independent from burst to burst). The initial mismatched channel estimation is based on the pseudo-inverse method performed on the 26-symbol CAZAC training sequence of the GSM burst as defined [18]. The structure of the communication chain is given Fig. 1 and the turbo-detector is based on Fig. 17. The channel coding is the same with scheme 1. Fig. 19 is for 8-PSK with interleaving depth of 2784 bits and 64-state SISO-DDFSE ($\nu_r = 2$), the transmitter filter being the linearized GMSK pulse shape and the receiver filter a root raise cosine filter with roll-off 0.5 (this low complexity receiver design can be used for the EDGE system). Fig. 20 is for GMSK with an interleaving depth of 928 bits and eight-state SISO-DDFSE ($\nu_r = 5$), the receiver filter being a six-pole butterworth with $BT = 0.6$ (this low complexity receiver design can be used for GSM system).

VII. Conclusion and Future Research Topics

In this paper, we have investigated several schemes for iterative decoding of encoded signals under multipath Rayleigh fading. The schemes, utilizing reduced complexity trellis search algorithms (SISO-DDFSE and SISO-PDFD) are especially appropriate for practical applications where higher order modulations (than BPSK) prohibit the implementation of the BCJR algorithm. The importance of such a study can be more pronounced if we consider the enhanced data rate TDMA systems (like EDGE) where eight-PSK is used to allow high data rates. Among the schemes proposed in this work, the most favorable one is the concatenation of an RSC code with a TCM which enables us to perform joint equalization and inner decoding using a SISO-PDFD algorithm. It has been demonstrated that such a scheme has a reasonable complexity and a very good performance on minimum phase channels where a prefilter is inserted at the receiver front-end to ensure that the equivalent channel response is minimum phase. The natural extension of this work is to study similar reduced-complexity iterative decoding schemes for nonminimum phase channels where prefiltering is not done.

The importance of channel reestimation is also studied in this paper. We have proposed two channel reestimation schemes (the EM and the Bootstrap algorithms) and compared their performances to that of the classical pseudo-inverse method. It has been shown that both of the proposed schemes perform much better than the pseudo-inverse method using 26-symbol CAZAC training sequence. Offering good performance at the expense of small additional complexity, the proposed channel reestimation algorithms can be implemented in turbo detection applications that are very sensitive to channel estimation errors. Particularly, the Bootstrap algorithm seems as a good tradeoff between performance and complexity.

Appendix

Considering that the random sequence $\mathbf{z}_1^\tau$ and random vector $\underline{\mathbf{h}}$ are independent random vectors, we can write the log likelihood of the complete data $\mathbf{w} = (\underline{\underline{\mathbf{\Theta}}}, \mathbf{z}_1^\tau)$ as

$$\ln p\left(\underline{\underline{\Theta}}, z_1^\tau \,|\underline{h}\right) = \ln p\left(\underline{\underline{\Theta}}|z_1^\tau, \underline{h}\right) + \ln p\left(z_1^\tau\right). \tag{44}$$

The second term is not a function of $\underline{h}$, so that it can be discarded. Since the decomposed noise processes are i.i.d, the first term can be split into

$$\ln p\left(\underline{\underline{\Theta}}|z_1^\tau, \underline{h}\right) = C - \frac{1}{N_0}\sum_{k=0}^{\nu_c}\frac{1}{\varsigma_k}\sum_{n=1}^{\tau}\left\|\theta_{n,k} - h_k z_{n-k}\right\|^2 \tag{45}$$

where C is a constant independent of $\underline{h}$. Expanding the term in $\|.\|^2$ and omitting the terms that do not depend on $\underline{h}$ leads to:

$$\ln, p\left(\underline{\underline{\Theta}}|z_1^\tau, \underline{h}\right) \sim -\frac{1}{N_0}\sum_{k=0}^{\nu_c}\frac{1}{\varsigma_k}\sum_{n=1}^{\tau}\left\{-2\Re e\left(\theta_{n,k}h_k^* z_{n-k}^*\right) + \left|h_k z_{n-k}\right|^2\right\}. \tag{46}$$

We now focus on the conditional expectation with respect to $\mathbf{w} = (\underline{\underline{\Theta}}, \mathbf{z}_1^\tau)$ where

$$E_{\mathbf{w}}\left\{\ln p\left(\underline{\underline{\Theta}}, \mathbf{z}_1^\tau \left|\underline{h}\right.\right)\left|y_1^\tau, \hat{\underline{h}}^{(\iota)}\right.\right\} = -\frac{1}{N_0}\sum_{k=0}^{\nu_c}\frac{1}{\varsigma_k}\sum_{n=1}^{\tau} \cdot E_{\mathbf{w}}\left\{-2\Re e\left(\theta_{n,k}h_k^*\mathbf{z}_{n-k}^*\right)+\left|h_k\mathbf{z}_{n-k}\right|^2\left|y_1^\tau, \hat{\underline{h}}^{(\iota)}\right.\right\} \tag{47}$$

can be explicitly derived as

$$\begin{aligned} &E_{\mathbf{w}}\left\{-2\Re e\left(\theta_{n,k}h_k^*\mathbf{z}_{n-k}^*\right)+\left|h_k\mathbf{z}_{n-k}\right|^2\left|y_1^\tau, \hat{\underline{h}}^{(\iota)}\right.\right\} \\ &= \sum_{s\in \mathrm{A}^{\nu_c+1}}\int_{\theta_{n,k}}\left\{-2\Re e\left(\theta_{n,k}h_k^* s_k^*\right)+\left|h_k s_k\right|^2\right\} \\ &\quad \cdot p\left(\theta_{n,k}\left|s, y_1^\tau, \hat{\underline{h}}^{(\iota)}\right.\right) \\ &\quad \cdot \Pr\left(\mathbf{z}_{n-\nu_c}^n = s\left|y_1^\tau, \hat{\underline{h}}^{(\iota)}\right.\right) d\theta_{n,k} \\ &= \sum_{s\in \mathrm{A}^{\nu_c+1}}\int_{\theta_{n,k}}\left\{-2\Re e\left(\overline{\theta}_{n,k}h_k^* s_k^*\right)\right\} \\ &\quad \cdot \Pr\left(\mathbf{z}_{n-\nu_c}^n = s\left|y_1^\tau, \hat{\underline{h}}^{(\iota)}\right.\right) \\ &\quad + \sum_{s\in \mathrm{A}^{\nu_c+1}}\left|h_k s_k\right|^2 \Pr\left(\mathbf{z}_{n-\nu_c}^n = s\left|y_1^\tau, \hat{\underline{h}}^{(\iota)}\right.\right) \end{aligned} \tag{48}$$

with

$$\mathbf{z}_{n-\nu_c}^n = \{z_n, \ldots, z_{n-\nu_c}\} \tag{49}$$

the symbol sequence or EM algorithm state at time n

$$s = \{s_0, \ldots, s_{\nu_c}\} \tag{50}$$

some possible realization in A^{ν_c+1} whose kth component is s_k, and

$$\overline{\theta}_{n,k} = \int_{\theta_{n,k}}\theta_{n,k}p\left(\theta_{n,k}\left|s, y_1^\tau, \hat{\underline{h}}^{(\iota)}\right.\right) d\theta_{n,k}. \tag{51}$$

Note that, due to the ISI Markovian structure, APPs on EM algorithm states $\mathbf{z}_{n-\nu_c}^n$ at time n are equal to APPs on underlying (complex-valued equivalent) ISI trellis states $\mathbf{z}_{n-\nu_c+1}^n$ at depth n. Observing that $\mathbf{z}_1^\tau$ and $\mathbf{y}_1^\tau$ are jointly Gaussian, we can rewrite the explicit expression of $\overline{\theta}_{n,k}$ as [28]

$$\overline{\theta}_{n,k} = h_k^{(\iota)}s_k + \varsigma_k\left[y_n - \sum_{m=0}^{\nu_c}\hat{h}_m^{(\iota)}s_m\right]. \tag{52}$$

The expression of the objective function $Q(\underline{h}|\hat{\underline{h}}^{(\iota)})$ is finally given by

$$\begin{aligned} &Q\left(\underline{h}\left|\hat{\underline{h}}^{(\iota)}\right.\right) \\ &= \frac{2}{N_0}\sum_{k=0}^{\nu_c}\frac{1}{\varsigma_k}\sum_{n=1}^{\tau} \cdot \Re e\left\{h_k^*\sum_{s\in \mathrm{A}^{\nu_c+1}}s_k^*\overline{\theta}_{n,k}\Pr\left(\mathbf{z}_{n-\nu_c}^n = s\left|y_1^\tau, \hat{\underline{h}}^{(\iota)}\right.\right)\right\} \\ &\quad - \frac{1}{N_0}\sum_{k=0}^{\nu_c}\frac{1}{\varsigma_k}\sum_{n=1}^{\tau}\left|h_k\right|^2\sum_{s\in \mathrm{A}^{\nu_c+1}}\left|s_k\right|^2 \\ &\quad \cdot \Pr\left(\mathbf{z}_{n-\nu_c}^n = s\left|y_1^\tau, \hat{\underline{h}}^{(\iota)}\right.\right). \end{aligned} \tag{53}$$

Q.E.D

REFERENCES

[1] C. Berrou, A. Glavieux, and P. Thitimajshima, "Near Shannon limit error correcting coding and decoding: Turbo codes," in *Proc. ICC'93*, Geneva, Switzerland, May 1993, pp. 1064–1070.

[2] C. Douillard, M. Jézéchiel, C. Berrou, A. Picart, P. Didier, and A. Glavieux, "Iterative correction of intersymbol interference: Turbo-equalization," *Eur. Trans. Telecommun.*, vol. 6, pp. 507–511, Sept. 1995.

[3] M. Mouly and M. B. Potet, *The GSM System for Mobile Communications*. Palaiseau, France: M. Mouly and M. B. Potet, 1992.

[4] A. Furuskar, S. Mazur, F. Muller, and H. Olofson, "EDGE, enhanced data rates for GSM and TDMA/136 evolution," *IEEE Pers. Commun. Mag.*, pp. 56–66, 1999.

[5] V. Franz and G. Bauch, "Turbo detection for enhanced data rate for GSM evolution," in *Proc., IEEE VTC99 Fall*, Amsterdam, The Netherlands, Sept. 1999.

[6] C. Berrou, P. Adde, E. Angui, and S. Faudeil, "A low complexity soft output Viterbi decoder architecture," in *Proc. ICC'93*, Geneva, Switzerland, May 1993, pp. 737–740.

[7] A. Glavieux, J. Laot, and J. Labat, "Turbo-equalization over a frequency selective channel," in *Proc. Int. Symp. Turbo Codes*, Brest, France, Sept. 1997.

[8] G. Bauch, H. Khorram, and J. Hagenauer, "Iterative equalization and decoding in mobile communications systems," in *Proc. EPMCC'97*, Bonn, Germany, Sept. 1997, pp. 307–312.

[9] G. Bauch and V. Franz, "A comparison of soft-in soft-out algorithms for turbo-detection," in *Proc. ICT*, vol. 2, Portos Carras, Greece, June 1998, pp. 259–263.

[10] L. R. Bahl, J. Cocke, F. Jelinek, and J. Raviv, "Optimal decoding of linear codes for minimizing symbol error rate," *IEEE Trans. Inform. Theory*, vol. IT-20, pp. 284–287, Mar. 1974.

[11] D. Raphaeli and Y. Zarai, "Combined turbo-equalization and turbo-decoding," *IEEE Commun. Lett.*, vol. 2, pp. 107–109, Apr. 1998.

[12] Y. Li and B. Chen, "Hybrid equalization for multipath fading channels with intersymbol interference," in *Proc. VTC'1999 Fall*, Amsterdam, The Netherlands, Sept. 1999, pp. 309–313.

[13] S. Benedetto, D. Divsalar, G. Montorsi, and F. Pollara, "Serial concatenation of interleaved codes: Performances, analysis, design and iterative decoding,", TDA Progress Rep. 42-126, Aug. 1996.

[14] S. Benedetto, G. Montorsi, and F. Pollara, "A soft-input soft-output APP module for iterative decoding of concatenated codes," *IEEE Commun. Lett.*, vol. 1, pp. 22–24, Jan. 1997.

[15] J. Hagenauer, E. Offer, and L. Papke, "Iterative decoding of binary block and convolutional codes," *IEEE Trans. Inform. Theory*, vol. 42, pp. 429–445, Mar. 1996.

[16] S. Benedetto, D. Divsalar, G. Montorsi, and F. Pollara, "Analysis, design, and iterative decoding of doubly serially concatenated codes with interleavers," *IEEE J. Select. Areas Commun.*, vol. 16, pp. 231–244, Feb. 1998.

[17] ETSI. GSM Recommendations 05.05, , Version 5.8.0, Dec. 1996.

[18] ETSI. GSM Recommendations 05.02, , Version 8–10, Nov. 1999.

[19] A. Duel-Hallen and C. Heegard, "Delayed decision-feedback sequence estimation," *IEEE Trans. Commun.*, vol. 37, pp. 428–436, May 1989.

[20] A. Wautier, J. C. Dany, and C. Mourot, "Filtre correcteur de phase pour égaliseurs sous-optimaux," *Ann. Telecommun.*, no. 9–10, 1992.

[21] M. V. Eyugoblu and S. U. Qureshi, "Reduced-state sequence estimation with set partitionning and decision feedback," *IEEE Trans. Commun.*, vol. 36, pp. 13–20, Jan. 1988.

[22] K. Kesolowski, "Efficient digital receiver structure for trellis-coded signals transmitted through channels with intersymbol interference," *IEE Electron. Lett.*, Nov. 1987.

[23] P. R. Chevillat and E. Eleftheriou, "Decoding of trellis-encoded signals in the presence of intersymbol interference and noise," *IEEE Trans. Commun.*, vol. 37, July 1989.

[24] R. Visoz, P. Tortelier, and A. O. Berthet, "Generalized Viterbi algorithm for trellis coded signals transmitted through broadband wireless channels," *Electron. Lett.*, vol. 36, no. 3, pp. 227–228, Feb. 2000.

[25] R. Visoz, A. O. Berthet, and P. Tortelier, "Joint equalization and decoding of trellis-encoded signals using the generalized Viterbi algorithm," in *Proc. IEEE VTC2000 Fall*, Boston, USA, Sept. 2000.
[26] V. Franz and G. Bauch, "Iterative channel estimation for turbo-detection," in *Proc. 2nd ITG Conf. Source and Channel Coding*, VDE/ITG, Mar. 1998, pp. 149–154.
[27] A. P. Dempster, N. M. Lain, and D. B. Rubin, "Maximum likelihood from incomplete data via EM algorithm," *J. Roy. Statist. Soc, Ser.*, vol. 39, pp. 1–38, 1977.
[28] M. Feder and E. Weinstein, "Parameter estimation of superimposed signals using EM algorithm," *IEEE Trans. Acoustics, Speech Signal Proc.*, vol. 36, pp. 477–489, Apr. 1988.

Antoine O. Berthet (M'00) was born in Paris, France, in 1974. He received the preliminary doctorate certificate in digital communication from Ecole Nationale Supérieure des Télécommunications de Paris (ENST) in 1997 and the engineer diploma from Institut National de Télécommunications (INT TELECOM) the same year. He is currently working toward the Ph.D. degree at ENST.

Since October 2000, he has been working for Alcatel Space Industries (ASPI), Nanterre, France. His research interests include coding theory, communication theory, and applications of the turbo principle in mobile and satellite environments.

Berna Sayrac Ünal (S'96–M'98) was born in Ankara, Turkey, in 1969. She received the B.S., M.S., and Ph.D degrees from the Department of Electrical and Electronics Engineering, Middle East Technical University (METU), Ankara, Turkey, in 1990, 1992, and 1997, respectively.

Between 1990 and 1999, she worked as a Research Assistant and as an Instructor at METU. Between 1999 and 2000, she was a Postdoc Fellow at France Telecom R&D, Issy Les Moulineaux, France. Currently, she is working as a Research Scientist at Philips Research France (PRF), Suresnes, France. Her research interests include mobile communications, coding theory, and information theory.

Raphaël Visoz was born in Grenoble, France, in 1972. He received the preliminary doctorate certificate in theoretical physics in 1995 and the diploma in 1997 from Ecole Nationale Supérieure des Télécommunications de Bretagne (ENSTB), Brest, France, including a Mobile communication specialization at Eurecom, Sophia antipolis, France. He is working toward the Ph.D. degree at the Ecole Nationale Supérieure des Télécommunications (ENST), Paris, France.

Since November 1997 he has been working for FTR&D (France Telecom Research and Development), France, Issy Les Moulineaux, in the field of third-generation (and beyond) mobile radio systems.